Journal of Engineering Technology Vol. 4:15-21, 2016(1)
ISSN 2231-8798

System and Link Level Performance of Pico and Macro-cells in 3D Extended Channel Models LTE-Advanced Networks

Zuhanis Mansor[1], Evangelos Mellios[2], Joe McGeehan[2], Geoffrey Hilton[2] & Andrew Nix[2]
[1]Section of Communication Technology
Universiti Kuala Lumpur British Malaysian Institute

[2]Centre for Communications Research, Department of Electrical & Electronic Engineering, University of Bristol Merchant Venturers Building, Woodland Road, Bristol, BS8 1UB, Bristol, United Kingdom

Corresponding email: zuhanis@unikl.edu.my

Abstract: This paper evaluates the user performance analysis at system level of pico-cells and macro-cells in 3D Extended Channel Models LTE-Advanced Networks. The analysis makes use of state-of-the-art 3D ray-tracing for a large number of macro and pico-cell base stations and user equipment locations. A baseband LTE-A link level simulator for 2x2 MIMO was designed and implemented in MATLAB to determine the user performance in pico-cells and macro-cells for line-of-sight and non-line-of-sight link. A pico-cell and macro-cell UE analysis at the system level and a comparison of external wall and lamp-post mounted pico-cell are also presented. User performance is analysed in terms of mean power, link budget and path loss coefficient. The empirical path loss equation for pico-cells and macro-cells in a HetNet urban environment are analyzed using 3D ray tracing data. The analysis shows that the user gains in terms of received power when the Pico base station is mounted on an external wall of a building rather than a lamp post. It can be determined that the deployment of pico-cells can be used to improve existing macro network coverage and performance in an LTE-Advanced network mostly near the cell edge.

Keywords: HetNets, Cellular networks, 3D-Channel Model, OFDMA, Downlink.

1.0 INTRODUCTION

Wireless communication technology has moved towards the development of digital technology. As the user density and various demands for services such as high-speed data, audio, video, seamless connectivity, service anytime and anywhere increases, it becomes much more complex to implement in real time. This is a key problem for future generation cellular technology. The problem with 3G networks is that they are struggling to meet consumer demand for data. Analysis of AT&T's data growth reveals that iPhone users, compared to other cell phone users, spend 25% less time talking and 21% more time accessing music, games and the internet [1]. The objective of 3G was to provide multi- rate, multimedia, cellular communications anytime and anywhere. From a link performance perspective, Long Term Evolution (LTE) already achieves data rates very close to the Shannon limit. Increasing the number of cells has always been the main means of adding capacity. As illustrated in Figure 1, mobile data traffic for smartphones, laptops and tablets is predicted to double each year from 2013 to 2018 [2]. 1000 times more capacity is predicted over 10 years period.

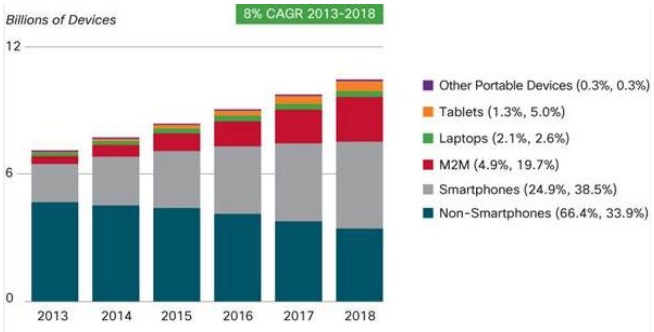

Figure Error! No text of specified style in document.**: The global mobile traffic forecast for 2010 to 2015 [2].**

According to the statistics [2], smartphones represented only 27% of total global handsets in use in 2013, but represented 95% of total global handset traffic. Since the data traffic demands in cellular networks are growing rapidly, significant improvements are now

required in spectral efficiency. In order to enhance peak data rates and overall network capacity, one of the most interesting solutions is to complement the macro layer with a number of low-power pico base stations, thereby forming a heterogeneous network (HetNet) [3–7]. The initial deployments of LTE consist of macro base stations (BS) and user equipment (UE) that caters for high mobility users. Thus, through HetNets a combination of macro and pico base stations can be used in order to increase the spectral efficiency per unit area in existing macro-cells.

This paper makes the following key contributions:

1. An analysis of pico and macro propagation for a 2x2 Spatial Multiplexing (SM) MIMO LTE-Advanced system in a HetNet scenario in terms of mean received power.
2. A pico-cell and macro-cell UE analysis at the system and link level in terms of link budget and path loss exponent.
3. A comparison of external wall and lamp-post mounted pico-cell BS deployments at link level.

Section 2 presents the system design and key parameters employed in this study. Section 3 describes the simulated data collection used. User performances evaluations are presented in Section 4 relative to mean power, mean SNR, pass loss, link budget and propagation model. Finally, conclusions are drawn in Section 5.

2.0 SYSTEM DESIGN AND KEY PARAMETERS

In this paper, a baseband LTE-A link level simulator for 2x2 MIMO was designed and implemented in MATLAB in order to analyse UE performance. Table 1 shows the key parameters of the LTE-A FDD downlink system used in this simulation. A channel bandwidth of 10 MHz and a carrier frequency of 2.6 GHz are assumed. All the physical layer parameters, unless explicitly stated, are listed in Table 1. Perfect channel estimation is used in the simulation. A packet size of 54 bytes is considered throughout the paper. In addition to that, 2000 channel realizations are considered in each simulation unless otherwise stated. A maximum of PER 10% is defined in order to evaluate area coverage. The chosen schemes are assumed to lie in outage if they exceed this PER limit.

The system noise temperature was 290K and a receive noise figure (NF) of 7dB was assumed at the UE [8]. The PER for each of the MIMO OFDMA PHY layer transmission modes is simulated as a function of SNR using MIMO channel data extracted from the 3D ray-tracing model. Three data modulation schemes are supported in the LTE-A system (QPSK, 16-QAM, and 64-QAM). The MCS considered in the simulation for 2x2 SM MIMO are given in Table 1. The achievable throughputs at the PHY layer can be calculated from the error free data rate and the residual packet error rate. An approximation for throughput is given by $Throughput = (1 - PER) \times R_b$, where the *Rb* represents the peak error-free transmission data rate and PER is the residual PER for a specific MCS mode.

The transmission date rate is defined as $R_b = N_{SS}(N_d r_c b N_s)/t_{slot}$, where N_{SS} denotes the number of spatial streams, N_d the number of data subcarriers, r_c the coding rate, b the number of coded bits per subcarrier, Ns is the number of OFDMA symbols per time slot and t_{slot} is the duration of the time slot. In order to perform link-level analysis in an efficient and scalable way, a PHY layer abstraction technique is required. The received bit mutual information rate (RBIR) abstraction technique is applied in this work to determine the optimal MCS mode.

Table Error! No text of specified style in document.**: DL Link Level Simulation Parameters**

Parameters	**Value**
Carrier Frequency	2.6 GHz
Transmission Bandwidth	10 MHz
Time Slot/Sub Frame Duration	0.5 ms /1 ms
Subcarrier Spacing	15 kHz
Sampling Frequency	15.36 MHz (4 x 3.84 MHz)
IFFT size	1024
Number of Occupied Subcarrier	600
Number of OFDMA/SC-FDMA symbols per time slot (Short CP)	7
CP Length (μs/samples)	(4.69/72) x 6, (5.21/80) x 1
Channel Knowledge	Perfect
Channel Estimation/Equalization	MMSE/MMSE
Subcarrier Mapping Scheme	Distributed (the bandwidth expansion factor of the symbol sequence, *Q*=4)
Channel Coding	Turbo
$N_{SS} \times N_{UE}$	2x2 SM (closed-loop)

3.0 SIMULATED DATA COLLECTION

In this paper, the work is implemented based on 23 macro base stations and 200 pico base stations. The propagation data for this study was made at 2.6 GHz in urban areas of central Bristol, (17.6 km²). After excluding all the UE rooftop locations, the above process resulted in 30,698 UE-Pico links and 9,492 Macro-eNB-UE links.

Journal of Engineering Technology Vol. 4:15-21, 2016(1)
ISSN 2231-8798

This large number of base stations was employed to ensure a statistically valid dataset. In practice, far fewer base stations are required by any single operator to provide effective coverage in this area. The propagation channel between each BS and UE is modelled as the spatial and polarimetric convolution of the antenna patterns with the spatial and temporal multipath components from our 3D outdoor ray-tracer [9]. In this investigation, Pico base station is mounted on the external walls of a building and on a lamp-post refer as Pico-eNB and Pico-LampPost respectively.

The BS makes use of horizontally spaced array elements while at the UE the elements are vertically spaced. The terms handset or UE, BS or Macro eNode B (Macro-eNB) and Pico eNode B (Pico-eNB) are used interchangeably in this paper. Figure 2 shows example macro-cell and pico-cell coverage maps based on the total average received signal power at the UE. Since macro-cells provide larger coverage areas than pico-cells, in the macro case it can be seen that there is less signal received at the cell-edge when compared to the picocell.

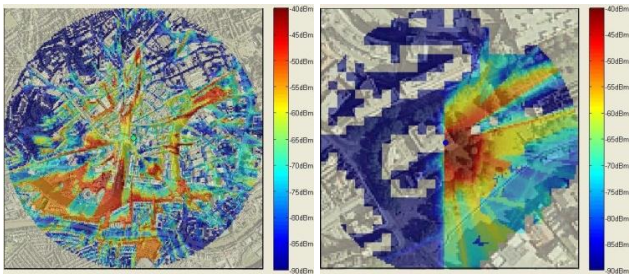

(a) Macro-cell **(b) Pico-cell**

Figure 2: Examples of coverage. a) Macro-cell. b) Pico-cell. Link colour indicates UE received signal strength: red implies strong, blue implies weak.

A detailed statistical analysis of the propagation parameters can be found in [9]. The method was used to compute a statistically valid set of wideband channel matrices suitable for Orthogonal Frequency Division Multiplexing (OFDM) modelling described in [10].The double-directional time-invariant channel impulse response h_{mn} for the m^{th} transmitting and n^{th} receiving antenna link is given by Eq. (1) [11], where $\delta(\cdot)$ represents the Dirac delta function, τ is the time-of-flight, $\Omega_{AoD}/\Omega_{AoA}$ represents the departure/arrival angle and L is the total number of multi-path components (MPCs).

$$h_{mn_L}(\tau,\Omega_{AoD},\Omega_{AoA}) = \sum_{l=1}^{L} h_{mnl}(\tau,\Omega_{AoD},\Omega_{AoA})$$
$$= \sum_{l=1}^{L} \mathrm{E}_{\mathrm{mnl}}\delta(\tau-\tau_l)\delta(\Omega_{AoD}-\Omega_{AoD,l})\delta(\Omega_{AoA}-\Omega_{AoA,l}) \quad (1)$$

where

$$\mathrm{E}_{\mathrm{mnl}} = \begin{bmatrix} E_{Tx,m}^{V} \\ E_{Tx,m}^{H} \end{bmatrix}^{T} \begin{bmatrix} a_l^{VV} e^{j\varphi_l^{VV}} & a_l^{VH} e^{j\varphi_l^{VH}} \\ a_l^{HV} e^{j\varphi_l^{HV}} & a_l^{HH} e^{j\varphi_l^{HH}} \end{bmatrix} \begin{bmatrix} E_{Rx,n}^{V} \\ E_{Rx,n}^{H} \end{bmatrix} \quad (2)$$

4.0 USER PERFORMANCE EVALUATION

I. This section presents the results that have been obtained from the LTE-A PHY layer simulation of a 2x2 DL SM MIMO OFDMA system. In particular, results focus on UE performance for LoS and NLoS locations. Results are summarized in the form of Cumulative Distribution Function (CDF) and complementary CDF graphs.

A. Performance Relative to Mean Power

In this section, user performance is given in pico-cells and macro-cells for Line-of-Sight (LoS) and Non- Line-of-Sight (NLoS) links based on the relative strength of the direct and scattered components (i.e. the K-factor), the RMS delay spread and the RMS AoD and AoA azimuth and elevation spreads of the UE signal. In addition, the user performance assuming 2x2 SM MIMO (LoS and NLoS) was evaluated for near-cell and cell-edge users for pico-cells and macro-cells, respectively. Figure 3 illustrates the relationship between the total mean received power (in dBm) and distance (in meters). Distances range from 5 m up to 150 m for pico-cells and 50m to 1km for macro-cells. In NLoS environments, it can be seen that the users are distributed mostly at the cell edge in pico-cells, compared to macro-cells. It can be seen from the figure that an increase in the BS-UE distance significantly decreases the mean power for both pico-cells and macro-cells.

For both picocell scenarios; Pico-Wall and Pico-LampPost, similar behavior is observed in LoS and NLoS. For instance, taking the maximum distance (at the cell-edge) from the analysis carried out for LoS, the mean power recorded in a pico-cell is -54 dBm and -52 dBm for Pico-Wall and Pico-LampPost, respectively. Furthermore, macro-cells have less mean received power (-59 dBm) (based on the three cases studied here). Meanwhile in NLoS, the minimum received power was -120 dBm in both pico-cells and macro-cells (this is the lowest power predicted by the Prophecy modelling tool).
If the average received power (dBm) and the UE Noise Figure (NF) are known then the mean SNR is given by the following equation:

$$\mathrm{SNR(dB)} = P_R(\mathrm{dBm}) - K_{Boltzmann}TB(\mathrm{dBm}) - NF(\mathrm{dB})$$

where $K_{\mathrm{Boltzmann}} = 1.38\times10^{-20} mWHz^{-1}K^{-1}$, and P_R is the average received power in dBm computed from a power sum of all arriving multipath components at each location.

Journal of Engineering Technology Vol. 4:15-21, 2016(1)
ISSN 2231-8798

T, *B*, and *NF* represent the temperature in Kelvin (*K*), the bandwidth in Hertz (Hz) and the noise figure (in dB) at the receiver, respectively. P_R and the corresponding BS-UE distances can be obtained from the ray tracing simulation data.

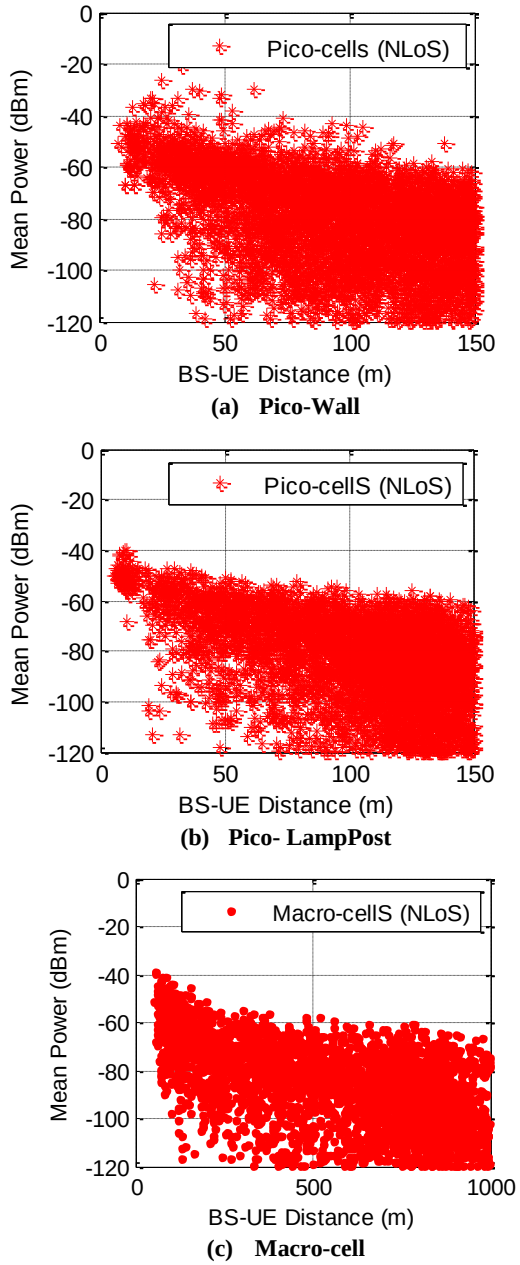

(a) Pico-Wall

(b) Pico- LampPost

(c) Macro-cell

Figure 3: Scatter plot of BS-UE distance versus mean received power for pico-cells and macro-cells with isotropic antennas in LoS (left) and NLoS (right). Data presented using the Bristol scenario

Figure 4 shows the CDF of the mean received power obtained for pico-cells and macro-cells in LoS and NLoS environments for Bristol and London. This figure also compares the mean received power for the picocell using Pico-Wall and Pico-LampPost assumptions. Significant loss in the mean received power is observed when moving from LoS to NLoS.

In LoS and NLoS scenarios, Pico-Wall produces the highest received powers compared to Pico-LampPost and macro-cells. It is interesting to note the UE gains in terms of received power when the Pico-eNB is mounted on an external wall of a building rather than a lamp post. In NLoS, the pico-cells and macro-cells in London have lower performance compared to Bristol. For example in Bristol the median Pico-Wall received power in NLoS is -78 dBm, while Pico-LampPost and macro-cells provide -81.2 dBm and -80dBm, respectively.

Whilst in the NLoS London scenarios, Pico-Wall achieved -73 dBm (median received power) and both Pico-LampPost and macro-cell achieved -74.7 dBm. Bristol achieved higher received powers than London for all cases. It can be seen that the maximum received power in the London scenario decreases by 12dB and 2dB for Pico-Wall and macrocell, respectively. Pico-LampPost is seen to generate the same values for London and Bristol.

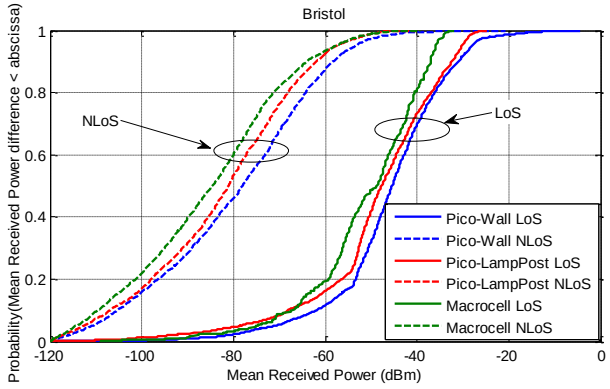

(a) Bristol

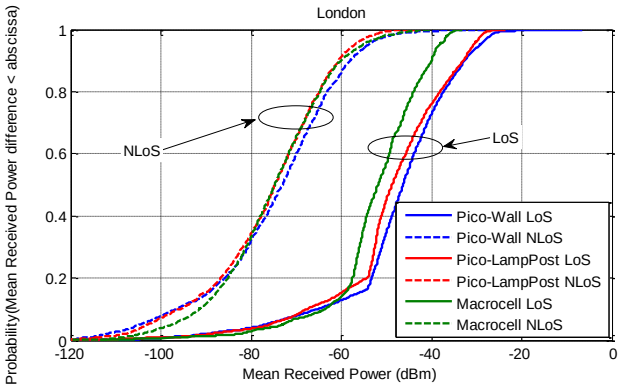

(b) London

Figure 4: CDF of mean received power for macrocell and picocell scenario in LoS and NLoS. Data generated using Bristol and London database**.**

B. Performance Relative to Link Budget and Propagation Model

This section presents a link budget analysis for the pico-cells and macro-cells based on the LTE-Advanced system. The received power can be determined by the transmitted power P_t, the antenna gains at the receiver G_r and transmitter G_t and the distance between the eNB and the UE. In this section, empirical path loss equations for pico-cells and macro-cells in a HetNet urban environment are developed from simulations conducted using a 3D outdoor ray-tracer in Bristol and London. An example of path loss in a pico-cell is shown in

Figure 5.

Figure illustrates the relationship between the mean path loss and the BS-UE distance for one of the Pico-eNB devices mounted on a lamp-post in Bristol. The UE lies in a LoS environment. In this analysis, path loss in dB is defined as the mean transmit power divided by the mean received power, where the antenna gain is already included in the measurement.

Error! Reference source not found.6 shows a scatter plot of the simulated path loss versus log-distance for the entire data set as a function of distance using 200 pico-cells and 23 macro-cells in Bristol. It compares the performance of macro-cell and pico-cell path loss in LoS and NLoS scenarios, where the Pico-eNB is mounted on the external walls of buildings (Pico-Wall) and on lamp-posts (Pico-LampPost). The path loss exponent varies depending on the carrier frequency, the BS & UE antenna height, and the environment types [12-15]. **Error! Reference source not found.** illustrates the mean path loss versus logarithmic UE-eNB separation distance for pico-cells and macro-cells in LoS and NLoS scenarios in Bristol and London. It can be seen that the macro-cells suffer more path loss compared to Pico-Wall and Pico-LampPost in LoS and NLoS scenarios.

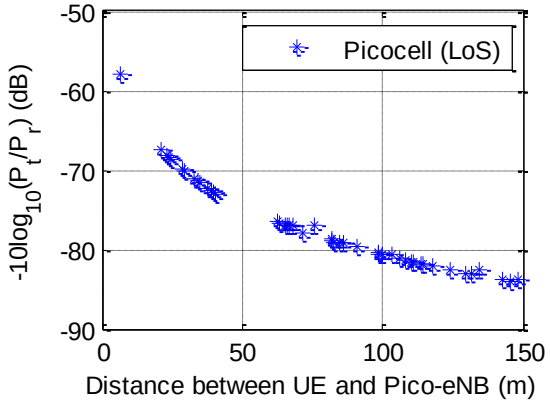

Figure 5: Scatter plot of mean path loss versus BS-UE separation distance for one of the 300 picocell sites in Bristol (Pico-eNB height = 5m).

In the LoS scenario, it can be seen that the mean path loss for Pico-Wall is less compared to Pico-LampPost. For instance, taking the maximum distance (at the cell-edge) in the LoS scenario in **Error! Reference source not found.**, it can be seen that Pico-Wall in Bristol achieves a gain of 2.3 dB over Pico-LampPost. However, in London there is no difference obtained between Pico-Wall and Pico-LampPost.

The difference between Pico-Wall and Pico-LampPost in terms of mean path loss performance is more noticeable in NLoS scenarios. The UE performance in Bristol at the cell-edge with Pico-Wall and Pico-LampPost is poor compared to London. In Bristol at the cell-edge, the Pico-Wall and Pico-LampPost show a loss in path loss performance of 6.8dB and 8.7dB, respectively. It can be seen that the London macro-cell achieves a gain of 2.8dB in LoS and 13.8 dB in NLoS compared to Bristol. A similar trend can be seen for the London deployment case.

Journal of Engineering Technology Vol. 4:15-21, 2016(1)
ISSN 2231-8798

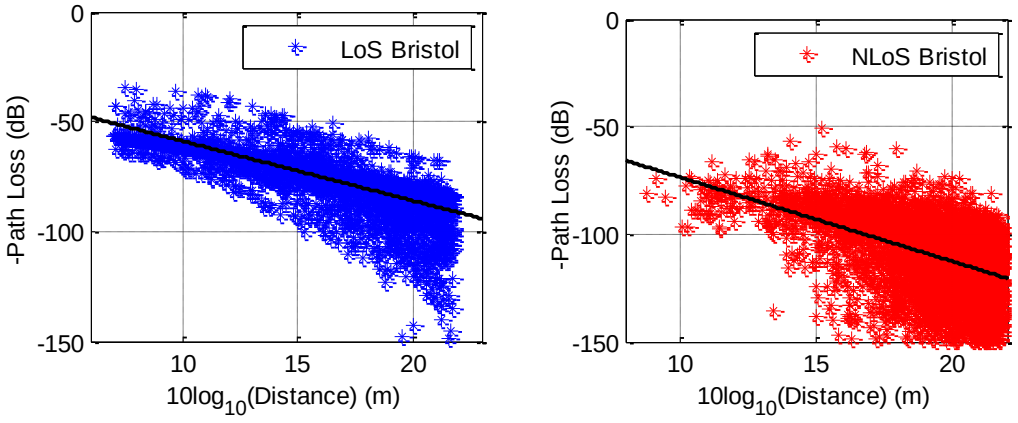

(a) Pico-Wall Bristol-NLoS

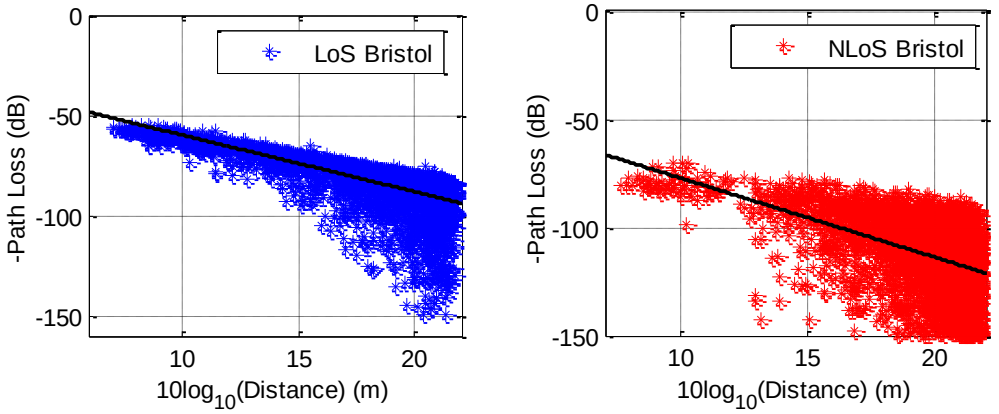

(b) Pico-LampPost Bristol

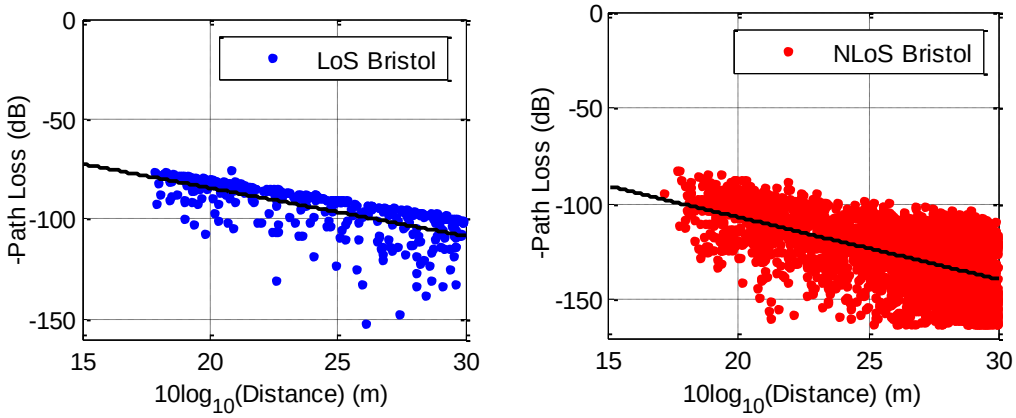

(c) Macro-cell Bristol

Figure 6: Path loss versus log distance for Bristol.

The path loss exponent η is obtained from the large spread of mean predicted path loss data in LoS and NLoS, for picocell and macrocell in Bristol and London, are summarized in Table 2. The results show the difference and similarity between pico-cells and macro-cells [Ray-Tracing Urban Macrocell Propagation Statistics and Comparison with Worldwide Initiative New Radio (WINNER) II/+ Measurements and Models paper].

In LoS cases, the obtained mean path loss exponents were higher for Pico-LampPost compared to Pico-Wall and macrocell in Bristol. However in the LoS London scenario, Pico-Wall achieved a high path loss exponent in all cases. Meanwhile in NLoS propagation links it can be seen that Bristol suffers higher path loss exponents compared to London for Pico-Wall, Pico-LampPost and macrocell respectively, probably due to the very hilly terrain of Bristol. This trend is reversed for LoS scenarios.

Table 2: Path loss exponent, η for pico-cells and macro-cells in LoS and NLoS links for a 2.6 GHz pico/macro HetNet scenario in Bristol.

	Bristol	
Scenario	LoS	NLoS
Pico- Wall	2.7	3.9
Pico- Lamp Post	2.8	3.6
Macrocell	2.4	3.2

5.0 CONCLUSIONS

This paper has presented a detailed propagation study for pico/macro SM MIMO handset performance based on a combination of site specific ray-tracing, polarmetric element patterns and simulation studies. The investigation was performed based on an ideal link with isotropic sources (polarisation independent) at the BS and UE. The Mean SNR was seen to vary between pico-cells and macro-cells. The UE in the picocell cases generally resulted in higher SNR and optimal throughput compared to the macrocell cases in NLoS environments. The analysis has shown that at high SNR, pico-cells can provide a higher capacity than macro-cells at the cell-edge. It can be determined that the deployment of pico-cells can be used to improve existing macro network coverage and performance in an LTE-Advanced network particularly near the cell edge.

ACKNOWLEDGEMENTS

Zuhanis Mansor would like to thank Professor Andrew Nix and Professor Joe McGeehan from University of Bristol, United Kingdom for the provision of laboratory facilities.

REFERENCES

[1] J. Hoadley and P. Maveddat, "Enabling small cell deployment with HetNet," *IEEE Wireless Communications*, vol. 19, no. 2, pp. 4–5, Apr. 2012.

[2] T. Cisco, "Cisco Visual Networking Index : Global Mobile Data Traffic Forecast Update, 2013 – 2018," Growth Lakeland, 2013.

[3] A. Khandekar, N. Bhushan, J. Tingfang and V. Vanghi, "LTE-Advanced: Heterogeneous networks," *European Wireless Conference (EW)*, pp. 978–982, 2010.

[5] J. Hoadley and P. Maveddat, "Enabling small cell deployment with HetNet," *IEEE Wireless Communications*, vol. 19, no. 2, pp. 4–5, Apr. 2012.

[6] S. Landström, H. Murai and A. Simonsson, "Deployment Aspects of LTE Pico Nodes," *Simulation*, 2011.

[7] K. Hiltunen, "Comparison of Different Network Densification Alternatives from the LTE Downlink Performance Point of View," in *IEEE Vehicular Technology Conference (VTC Fall)*, pp. 1–5, 2011.

[8] H. Holma and A. Toskala, *LTE for UMTS OFDMA and SC-FDMA Based Radio Access*. John Wiley & Sons, Ltd, 2009.

[9] E. Mellios, A. R. Nix and G. S. Hilton, "Ray-tracing urban pico-cell 3D propagation statistics for LTE heterogeneous networks," *7th European Conference on Antennas and Propagation (EuCAP)*, April 2013.

[10] Y. Q. Bian, A. R. Nix, E. K. Tameh and J. P. McGeehan, "MIMO–OFDM WLAN Architectures, Area Coverage, and Link Adaptation for Urban Hotspots," *IEEE Transactions on Vehicular Technology*, vol. 57, no. 4, pp. 2364–2374, Jul. 2008.

[11] M. Steinbauer, A. F. Molisch and E. Bonek, "The double-directional radio channel," *IEEE Antennas and Propagation Magazine*, vol. 43, no. 4, pp. 51–63, 2001.

[12] S. Y. Seidel, T. S. Rappaport, S. Jain, M. L. Lord and R. Singh, "Path loss, scattering and multipath delay statistics in four European cities for digital cellular and microcellular radiotelephone," IEEE Transactions on Vehicular Technology, vol. 40, no. 4, pp. 721–730, 1991.

[13] S. Y. Seidel, T. S. Rappaport, S. Jain, M. L. Lord and R. Singh, "Path loss, scattering and multipath delay statistics in four European cities for digital cellular and microcellular radiotelephone," IEEE Transactions on Vehicular Technology, vol. 40, no. 4, pp. 721–730, 1991.

[14] P. Harley, "Short distance attenuation measurements at 900 MHz and 1.8 GHz using low antenna heights for microcells," IEEE Journal on Selected Areas in Communications, vol. 7, no. 1, pp. 5–11, 1989.

[15] T. J. Harrold, A. R. Nix and M. A. Beach, "Propagation studies for mobile-to-mobile communications," IEEE 54th Vehicular Technology Conference. VTC Fall, vol. 3, pp. 1251–1255, 2001.

[16] Z. Mansor, E. Mellios, A. Nix, J. McGeehan and G. Hilton, "Impact of antenna patterns and orientations in heterogeneous LTE-Advanced networks," *6th European Conference on Antennas and Propagation (EUCAP)*, pp. 1904–1908, 2012.